IEEE Access
Multidisciplinary ⋮ Rapid Review ⋮ Open Access Journal

Received January 3, 2021, accepted January 7, 2021, date of publication January 12, 2021, date of current version January 20, 2021.

*Digital Object Identifier 10.1109/ACCESS.2021.3051063*

# Improving Wind Turbine Pitch Control by Effective Wind Neuro-Estimators

**J. ENRIQUE SIERRA-GARCÍA**[1] **AND MATILDE SANTOS**[2]
[1]Department of Electromechanical Engineering, University of Burgos, 09006 Burgos, Spain
[2]Institute of Knowledge Technology, Complutense University of Madrid, 28040 Madrid, Spain

Corresponding author: J. Enrique Sierra-García (jesierra@ubu.es)

This work was supported in part by the Spanish Ministry of Science, Innovation and Universities through MCI/AEI/FEDER under Project RTI2018-094902-B-C21.

**ABSTRACT** Data about wind are usually available from different databases, for different locations. In general, this information is the average of the wind speed over time. The wind reports are crucial for designing wind turbine controllers. But when working with floating offshore wind turbines (FOWT), two problems arise regarding the wind measurement. On the one hand, there are no buoys at deep sea, but near the coast where the wind is not so strong neither so stable; so the measurements do not fully correspond to reality. On the other hand, these floating devices are subjected to extreme environmental conditions (waves, currents, . . .) that produce disturbances and thus may distort wind measurements. To address this problem, this work presents a novel pitch neuro-control architecture based on neuro-estimators of the effective wind. The control system is composed of a proportional-integral-derivative (PID) controller, a lookup table, a neuro-estimator, and a virtual sensor. The neuro-estimator is used to estimate the effective wind in the FOWT and to forecast its future value. Both current and future wind signals are combined and power the controller. The virtual sensor also provides a measure of the effective wind based on other available signals related to the wind turbine, such as the pitch angle and the angular velocity of the generator. Neural networks are trained online to adapt to changes in the environment. Intensive simulations are carried out to validate the effectiveness of this neuro control approach. Controller performance is compared to a PID, obtaining better results. Indeed, an improvement of 16% for sinusoidal wind and an average improvement of 8% are observed.

**INDEX TERMS** Floating offshore wind turbines (FOWTs), pitch control, neuro-estimator, neural network, virtual sensor, wind energy.

## I. INTRODUCTION

Achieving the Paris Climate Goals [1] requires significant acceleration in a variety of sectors. Among renewable energies, wind and solar resources seem to be leading the transformation of the global electricity grid. It is estimated that onshore and offshore wind power will generate more than a third (35%) of total electricity needed in the medium term, becoming the main source of generation by 2050 [2]. For these predictions to come true, some engineering challenges related to wind turbines (WT) must be still addressed.

An area of new challenges related to wind energy is automatic control. In addition to energy efficiency of the turbine itself, other control objectives are key to the develop of this wind technology: stabilization of the output power around its nominal value, maximization of the energy, vibrations damping, reduction of fatigue in the structure, etc. Even more, these objectives must be guaranteed in all operating conditions, which in the case of floating offshore wind turbines (FOWT) can be very demanding. Moreover, it has been shown that the control system can affect the stability of the floating device [3].

Different control actions have been proposed to achieve these goals. Structural control may help to reduce vibrations and thus, fatigue and maintenance. Pitch angle, generator speed, and yaw control are in charge of improving the performance of the turbine. The pitch control modifies the angle of attack of the wind and is generally used to keep the output power at its nominal value, once the wind exceeds certain wind speed threshold. Controlling the angular velocity of the generator is typically used to track the optimal rotor speed to maximize power when the wind is below that cut-off speed. The yaw control modifies the orientation of the nacelle to match the direction of the wind. The complexity of

The associate editor coordinating the review of this manuscript and approving it for publication was Dipankar Deb.

this system has led to exploring the usefulness of intelligent control techniques such as fuzzy logic, neural networks and reinforced learning, among others, to address WT control problems [4], [5].

### A. MOTIVATION AND MAIN CONTRIBUTIONS

Wind information is key to analyze the performance of a wind turbine and improve its control. This knowledge is usually available from different databases, for different locations. In general, this information is the average of the wind speed over time. But this information may not be so reliable, particularly in the case of floating offshore wind turbines. This is due to the fact that, on the one hand, there are no buoys at deep sea, but near the coast where the wind is not so strong neither so stable; so the measurements do not fully correspond to reality. In addition, these floating devices are subjected to extreme environmental conditions (waves, currents, ...) that produce disturbances and thus may distort wind measurements.

Therefore, in this work the issue of how to handle the disturbances in the wind measurements is addressed.

We propose a neuro control approach that is able to deal with external and internal uncertainties. External uncertainties are included in the model as external disturbances. For instance, the ocean waves influence the inclination of the floating wind turbine. This makes the wind that impacts the rotor different from the one measured. That is why what we called the effective wind is calculated using a neuro-estimator. This way, the disturbance of the waves is included and can be tackled. In fact, in this proposal we not only estimate the current effective wind but the forecasting effective wind. Both values, estimation and prediction, are combined and used to compensate the mismatches of the wind measurements.

On the other hand, internal uncertainties that may come from the model are considered by the virtual sensor that is part of the control scheme. These uncertainties are considered as a bias in the effective wind estimation. Thus, they are also handled by the lookup table of the control strategy when the pitch reference is generated and are then compensated.

Hence, the main contributions of this work can be summarized as follows.

- A neuro-estimator is designed to estimate the current effective wind that impacts the turbine, in spite of external disturbances. This neural network also forecasts the future effective wind using online learning.
- A virtual sensor has been also implemented to measure the effective wind based on internal measures of the turbine.
- A pitch control architecture is proposed to stabilize the power output around its nominal value. The control strategy combines the neuro-estimator, a PID controller, the virtual sensor and a lookup table.
- This control approach has been validated through intensive simulations under the presence of disturbances that affects the wind measurement. It has been compared with simpler control configurations with satisfactory results.

After this section, where the motivation and main contributions of the paper are stated, the rest of the paper is organized as follows. Section II describes the related works. Section III presents the mathematical model of the wind turbine used and how the disturbances are represented. The neuro-controller, the neuro-estimator and the virtual sensor are designed in Section IV. Simulation results are discussed in Section V. The paper ends with the conclusions and future works.

## II. RELATED WORKS

The improvement in the efficiency of the wind turbines comes from the hand of the automatic control. That is why there are numerous papers in the literature that have addressed this problem, with different approaches. Among them, intelligent techniques have been proved to be useful for these complex and non-linear systems. In [6], a review of applications of artificial intelligent algorithms in wind farms is presented. In this paper, several issues in wind farms are studied, namely: wind farm controllers, Mach number, wind speed prediction, wind power prediction and other problems of wind farms are reviewed. Two future research directions are pointed out to be developed by artificial intelligent algorithms: wind farm control systems, and wind speed and power prediction. Both topics are addressed in our paper.

Regarding wind turbine control, a good survey on the application of expert systems in pitch control is found in [7]. It presents a review on expert systems developed in recent years to offer control solutions that approximate the conditions of different wind turbines. To develop an expert control system is not only necessary to know the dynamic operation of the system, but also to anticipate the control response to each of the different likely but uncertain scenarios.

In [4], a neural controller based on radial basis function neural networks is used for pitch control. An unsupervised learning algorithm is implemented that allows the neural network to adjust the proper control law to stabilize the output power around the rated power and to reduce the mean squared error over time. The neuro-control has been compared with a traditional controller, giving better results. Rubio *et al.* [8] present a fuzzy-logic based system for the pitch control of a wind turbine installed on a semi-submersible platform. They work with different wind speed and turbulences, but with the same wind uniform profile. The intelligent controller has been compared to results obtained by the PI that NREL proposes as reference for the controller of the type of floating wind turbine they are working with. The performance obtained is clearly superior, particularly for winds above the nominal value. In addition, the fuzzy control system could take into account different operating conditions, such as aspects related to the environment. In [9] a hierarchical fuzzy logic controller is designed to solve the nonlinear system effects produced by atypical winds. It proposes to

install a wind speed measurement system at a calculated distance where the movement of the mechanical system of the pitch angle will anticipate the position of the setpoint angle, in order to minimize the effects of the wind gust on the rotation of the turbine. In [10], a novel fuzzy rule is proposed to adopt a positive pitch strategy when the error between the measured and rated generator speed becomes large and continues to increase, and to adopt a negative pitch strategy when the error is small. This intelligent fuzzy pitch control not only reduces the power deviation but also decreases some ultimate loads and fatigue of the tower base and the blade root.

A specific challenge of wind turbines in general, and of floating offshore wind turbines in particular, is the wind forecasting and the disturbance in the measurement of wind speed [11], [12]. As it is well known, the output power generated by a wind turbine is directly related to the wind speed. Therefore, the use of wind information can improve the performance of WT controllers. However, WTs, and especially FOWTs, can be subjected to harsh external conditions, such as oscillations produced by ocean waves that distort the wind measurement [3]. To face this problem, in the work here presented the use of a neural network based estimator is proposed to estimate the effective wind speed and forecast the future wind velocity. Estimation of wind speed and disturbances has received attention in other works. In the paper by Asghar and Liu [11], an effective wind speed estimator is proposed using an adaptive neuro-fuzzy algorithm (ANFIS). Authors try to obtain the relationship of the wind speed with the tip speed ratio (TSR), rotor speed and mechanical power. The ANN trains the fuzzy membership functions of the inputs using least square and apply back propagation gradient descent to accurately estimate the effective wind speed without using any mechanical wind speed sensor. Then, the estimated effective wind speed and the optimal TSR are used to design an optimal rotor speed estimator. These estimators are implemented in simulation to verify their performance. The results show the accuracy and reliability of both estimators. In a similar paper by the same authors, [13], a hybrid intelligent learning adaptive neuro-fuzzy inference system is proposed to estimate the Weibull wind speed probability distribution. Results are compared with five well-known numerical methods. Both papers address the problem of selecting the most efficient and economically viable wind turbine, and for this purpose, they analyse four small scale wind turbines.

Deng *et al.* present an optimal rotor speed controller that uses an observer-provided estimate of effective wind speed [14]. This effective wind speed is estimated from the measured rotor speed, the measured pitch angle, and the observed aerodynamic torque by the disturbance observer. Some simulation results validate the availability of the improved effective wind speed estimation algorithm and the control strategy for capturing maximum wind energy. In a previous work [15], the same authors propose a sensorless effective wind speed estimation algorithm based on the unknown input disturbance observer and the extreme learning machine for the variable-speed wind turbine. The proposed algorithm is validated by simulation studies on a medium size variable-speed wind turbine and compared with the Kalman filter-based method with satisfactory results.

In [16], an artificial neural network-based reinforcement learning (RL) for WT yaw control is presented. As it is well known, one of the main drawbacks of yaw angle control is that it requires a correct measuring of the incoming wind direction. Otherwise the positioning of the nacelle will be incorrect and the system will not be able to maximize the wind power. To solve this issue, authors apply RL to achieve some knowledge of the yaw control system of the wind turbine that ensures that, after some time, the best action in a certain situation is taken in an automatic way.

Recently, deep learning has been used to estimate the wind turbine angular velocity remotely [17]. In this paper it is investigated how the forecast/prediction models of the existing wind farms can be adapted to generate a prediction model for new stations.

Not so closely related but focused on an interesting topic, a recent paper by Dhiman and Deb (2020) deals with wind forecasting in wind farms, considering error in the wind speed prediction. In this case this prediction is applied to wake management in order to reduce the operational cost of a hybrid wind farm equipped with battery energy storage systems [18]. The same authors have another paper where they study the wind speed prediction in presence of wake effect [19]. The goal of this paper is the optimal placement of turbines in a wind farm. The interesting result is how they conclude that the wake effect reduces the effective wind power capture. With the same objective, a parametric study of the wake effect on the estimation of the energy production in wind farms is presented in [20].

On the other hand, although it is out of the scope of this work, it could be worthy to present some practical issues related to the wind turbines, mainly with wind farms. Just to mention a few of them. The control of the wind turbines generator, usually a double fed induction one, has been widely studied. For instance, Mohamed *et al.* [21], based on a simplified model for the frequency response of DFIG WT, develop an adaptive model predictive controller for the load frequency control of the power system of the WT.

Interestingly, the uncertainty that is inherently associated with the operation of a wind turbine should be also considered from the economic point of view, as Mohamed *et al.* proposes in [22]. In this paper, authors apply the transmission switching integrated interval robust chance-constrained (TSIRC) approach as an effective tool to model the uncertainties of the wind units by increasing the wind park-energy storage system (WPES) profit as a strategic producer while reducing the system operation cost. They work with a 24-h time horizon, in a day ahead electricity market. In a similar way, the stochastic nature of the environment is taken into account in [23], where an information management system for a wind power producer is proposed. In this case, it also has an energy

storage system and participates in a day-ahead electricity market.

As shown, previous works that estimate the effective wind speed and use it in the controller are scarce. In addition, there are still some interesting and novel aspects that can be studied further. For example, none of the previous papers explored the combination of the current and predicted future effective wind.

## III. MATHEMATICAL MODEL OF THE WIND TURBINE AND THE DISTURBANCES

In this work a model of a small 7 kW wind turbine is used. It represents a real wind turbine. The equations of the model are summarized in (1-8). The development of these equations can be found in [4], [24].

$$\dot{I}_a = \frac{1}{L_a}\left(K_g \cdot K_\phi \cdot w - (R_a + R_L) I_a\right), \tag{1}$$

$$\lambda = (w \cdot R)/v_{ef}, \tag{2}$$

$$\lambda_i = \left[\left(\frac{1}{\lambda + c_8}\right) - \left(\frac{c_9}{\theta^3 + 1}\right)\right]^{-1}, \tag{3}$$

$$C_p(\lambda_i, \theta) = c_1\left[\frac{C_2}{\lambda_i} - c_3\theta - c_4\theta^{c_5} - c_6\right] e^{-\frac{c_7}{\lambda_i}}, \tag{4}$$

$$\dot{w} = \frac{1}{2 \cdot J \cdot w}\left(C_p(\lambda_i, \theta) \cdot \rho\pi R^2 \cdot v_{ef}^3\right) - \frac{1}{J}\left(K_g \cdot K_\phi \cdot I_a + K_f w\right), \tag{5}$$

$$\ddot{\theta} = \frac{1}{T_\theta}\left[K_\theta\left(\boldsymbol{\theta_{ref}} - \theta\right) - \dot{\theta}\right], \tag{6}$$

$$\boldsymbol{P_{out}} = R_L \cdot I_a^2 \tag{7}$$

where $L_a$ is the armature inductance (H), $K_g$ is a dimensionless constant of the generator, $K_\phi$ is the magnetic flow coupling constant (V· s/rad), $R_a$ is the armature resistance ($\Omega$), $R_L$ is the resistance of the load ($\Omega$), considered in this study as purely resistive; $w$ is the angular rotor speed (rad/s), $I_a$ is the armature current (A), and $\lambda$ is the tip-speed ratio which is dimensionless.

The values of the coefficients $c_1$ to $c_9$ that define the power coefficient $C_p$ depend on the characteristics of the wind turbine; $J$ is the rotational inertia (Kg.m$^2$), $R$ is the radius or blade length (m), $\rho$ is the air density (Kg/m$^3$), $K_f$ is the friction coefficient (N.m/rad/s), $K_\theta$ and $T_\theta$ are dimensionless parameters of the pitch actuator, $v_{ef}$ is the effective wind velocity in the blades (m/s), $v_M$ is the wind velocity measured by an anemometer sensor, and $d_W$ is the disturbance function.

The state variables of the system are the current in the armature, the angular rotor speed, the pitch angle and the pitch velocity. The main variable of the control problem here addressed is the pitch acceleration, where $\theta$ is the pitch angle (rad) and $\theta_{ref}$ is its reference (rad). Indeed, the controller proposed in this paper is applied to find the pitch reference signal, $\theta_{ref}$, that stabilize the output power, $P_{out}$, of the wind turbine around its rated value.

### A. DESCRIPTION OF THE DISTURBANCES

Offshore wind turbines are subjected to external disturbances which may produce oscillations in the tower, nacelle and/or the hub. Because of that, the effective wind $v_{ef}$, which is transformed into mechanical power, does not perfectly match with the wind speed measured by the anemometer sensor. This difference has been considered and modelled in this work as a disturbance, $d_W$.

$$v_{ef} = d_W(v_M) \tag{8}$$

The procedure to obtain the effective wind $v_{ef}$ from the measured wind $v_M$ must include the uncertainty in the measurements. Two sources of uncertainty have been considered. First, an external disturbance produced by the movement of the wind turbine, $d_{Wext}$. This motion makes the wind reaching the blades different from the measured one. In addition, the aerodynamic shape of the blades changes the effective wind $v_{ef}$ that feeds the hub. The latter issue is not always well-known and introduces uncertainty. It has been here modelled as an internal disturbance, $d_{Wint}$.

Considering the behavior of the regular ocean waves as periodic, the external disturbance has been modelled as a sinusoidal signal with white gaussian noise.

$$d_{W_{ext}}(v_M) = v_M + A_d \cdot \sin\left(\frac{2\pi}{T_d} \cdot t\right) + A_d \cdot K_d rand(t) + C_d \tag{9}$$

where $A_d$ is the amplitude of the disturbance in m/s, $T_d$ is the period of the wave, $C_d$ is a constant term, $K_d$ is a coefficient to adjust the signal noise ratio, and $rand()$ denotes the random function.

The wind produces ocean waves with periods between 0.1 s to 300 s [25]. So, we have considered these values in the experiments. Storms and earthquakes produce waves with longer periods but they have not been tested in this work.

On the other hand, the internal disturbance has been modelled by two filters placed in cascade (10-11).

$$filt_1(s) = \frac{\beta \cdot s + \sqrt{2}}{\beta^2 \cdot s^2\left(\sqrt{\left(\frac{2}{\alpha}\right)} + \sqrt{\alpha}\right) \cdot \beta \cdot s + \sqrt{2}} \tag{10}$$

$$filt_2(s) = \frac{\gamma \cdot s + 1/\tau}{s + 1/\tau} \tag{11}$$

where $[\alpha, \beta, \gamma, \tau]$ values are $[0.55, 0.832, 1.17, 9]$. Then,

$$d_{W_{int}}(s) = filt_1(s) \cdot filt_2(s) \tag{12}$$

Finally, combining equations (9) and (12) the effective wind can be modelled by:

$$v_{ef} = d_{W_{int}}(d_{W_{ext}}(v_M)) \tag{13}$$

## IV. DESIGN OF THE NEURO-CONTROLLER

The architecture of the neural controller is shown in Figure 1. A lookup table (green block) obtains a pitch reference $\theta_{TAB}$ as a function of the estimated wind. The mapping between

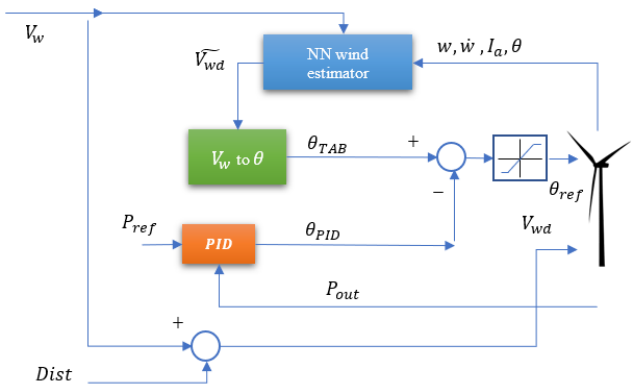


**FIGURE 1.** Architecture of the neural controller.

the wind and the pitch reference that gives the corresponding rated power is not perfect. Thus, to reduce this mapping error we use a PID with anti-windup regulator. This conventional controller is still the most widely applied to real wind turbines, although a more advanced controller could be used.

The PID controller calculates the difference between the power output $P_{out}$ and the power reference, $P_{ref}$, and uses it to generate $\theta_{PID}$. Then, both references, $\theta_{TAB}$ and $\theta_{PID}$, are combined and then limited to ensure the total pitch reference $\theta_{ref}$ does not overpass the pitch limits $[0, \pi/2]$ rad. As it will be shown in the experimental results, the PID smoothers the pitch reference generated by the lookup table. The WT has as inputs the pitch reference from the controller, $\theta_{ref}$, and the wind speed with the external disturbance, $V_{wd}$.

The NN wind estimator receives the angular rotor speed $w$ and its derivative $\dot{w}$, the pitch angle $\theta$, and the current in the generator, $I_a$. This neural system then estimates the effective wind and the disturbance in the current control interval, as well their values for the next control interval. The estimated and predicted winds are weighted and the result, $\widetilde{V_{wd}}$, is used as input of the lookup table.

The following equations formally describe the behavior of the controller (14-19).

$$V_{ACT}(t_i) = f_{NACT}(w(t_{i-1}), \dot{w}(t_{i-1}), I_a(t_{i-1}), \theta(t_{i-1}), V_w(t_i)) \quad (14)$$

$$V_{FUT}(t_i) = f_{NFUT}(w(t_{i-1}), \dot{w}(t_{i-1}), I_a(t_{i-1}), \theta(t_{i-1}), V_w(t_i)) \quad (15)$$

$$\widetilde{V_{wd}}(t_i) = \begin{cases} V_w(t_i) & t \le t_{onl} \\ K_{ACT} \cdot V_{ACT}(t_i) + K_{FUT} \cdot V_{FUT}(t_i) & t > t_{onl} \end{cases} \quad (16)$$

$$\theta_{TAB}(t_i) = f_{LT}(\widetilde{V_{wd}}(t_i)) \quad (17)$$

$$\theta_{PID}(t_i) = Kp_c \cdot P_{err} + Kd_c \cdot \frac{d}{dt} P_{err} + Ki_c \int P_{err} \cdot dt \quad (18)$$

$$\theta_{ref}(t_i) = MIN(\pi/2, MAX(0, \theta_{TAB}(t_i) - \theta_{PID}(t_i))) \quad (19)$$

where $f_{NACT}$ and $f_{NFUT}$ are the functions of the neural networks which estimate and predict the current and the future effective wind, respectively; $K_{ACT}$ and $K_{FUT}$ are coefficients within the range [0, 1] that fulfil the constraint $0 \le K_{ACT} + K_{FUT} \le 1$; $f_{LT}$ denotes the function of the lookup table, and $[Kp_C, Kd_c, Ki_c] \in \mathbb{R}^3$ are the tuning parameters of the PID controller. The parameters $K_{ACT}$ and $K_{FUT}$ are used to ponder the importance given to the forecasted wind respect to the current estimated wind.

The lookup table implements a mapping function between the wind speed and the pitch reference. The larger the wind speed, the bigger the pitch angle, in order to stabilize the output power around its rated value. This table can be defined by experimental data or by airflow simulation tools. In our case, the data of the table have been obtained introducing different constant wind speed values in the simulation model and adjusting the pitch reference to obtain the rated power. This mapping function is shown in Figure 2.

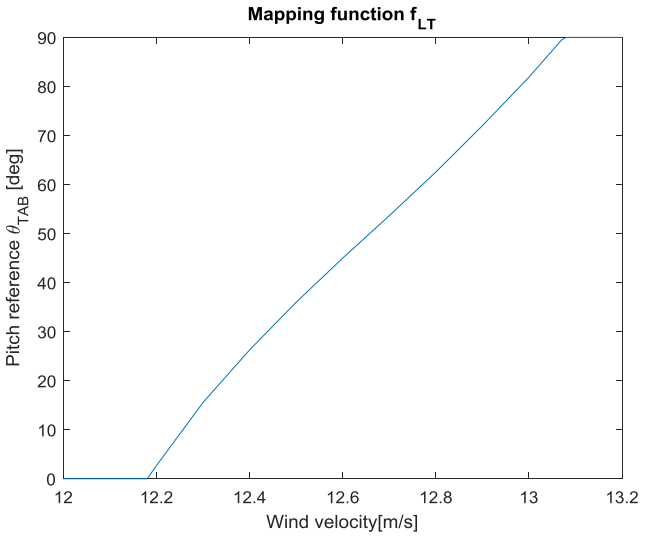


**FIGURE 2.** Mapping function implemented by the lookup table.

### A. DESCRIPTION OF THE NEURO-ESTIMATOR

In this section we focus on the estimation of the present wind velocity, $V_{ACT}$ and on the forecasting of the future wind speed, $V_{FUT}$. As it is shown in Figure 3, the neuro-estimator is formed by two neural networks, which calculate $V_{ACT}$ and $V_{FUT}$, plus a virtual sensor, that provides information to train the networks, a memory buffer, and some switches to commute signals.

Particularly, the effective wind virtual sensor calculates a measurement of the effective wind based on the angular speed of the generator, its derivative, the current in the armature, the pitch and the measured wind speed. This measurement, $V_{vs}$, is used to train the neural networks ACT and FUT (Figure 3). According to (16), before $t_{onl}$ time, the estimator is not used because the neural networks have not been trained. When $t = t_{onl}$, the switches SW1, SW2 and SW3 are set to the modes [“down”, “up”, “up”] and the neural networks are trained. The inputs of NN-FUT go through a memory buffer to allow the neural network to associate the inputs at $t_i$ with the output at $t_{i+2}$.

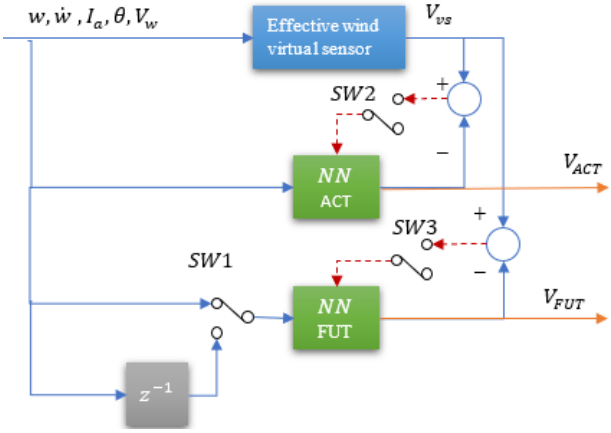


**FIGURE 3.** Architecture of the neuro-estimator.

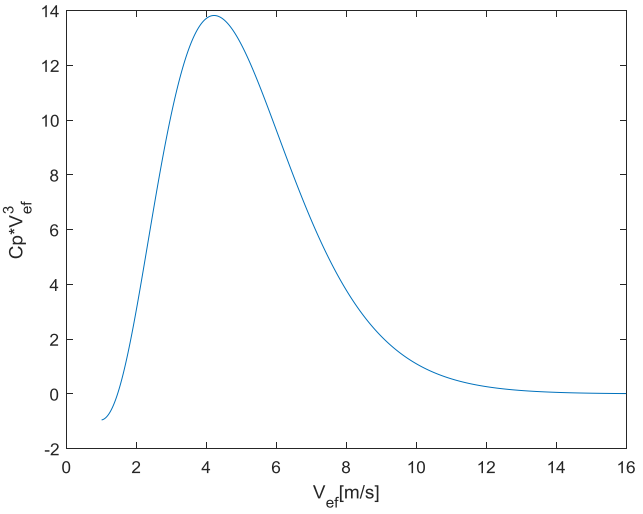


**FIGURE 4.** $C_p(\lambda_i, \theta)\cdot v_{ef}^3$ for $\theta$ =0 rad and $w$ =5.4 rpm.

Once the neural networks are already trained the estimator commutes each control period between two states: estimation and online-learning. During the estimation the switches SW1, SW2 and SW3 must be set to the configuration [''up'', ''down'', ''down'']. This way $V_{ACT}$ and $V_{FUT}$ are calculated using equations (14) and (15). After that, the switches change to [''down'', ''up'', ''up''] and the weights of the neural networks are updated by the learning algorithm.

In the experiments, feedforward neural networks with two hidden layers and 3 neurons per layer were applied, although a different network configuration could have been used. The Levenberg-Marquardt backpropagation algorithm has been used for the training.

The utility of these neural networks is twofold. On the one hand, NN-ACT allows to estimate the effective wind in case the virtual sensor cannot provide a real value (singularities such as division by 0, square roots of negative values, etc.) In these cases the neural networks still provide an estimation of input values different to the ones used during the training. This is, the neural networks generate new knowledge. On the other hand the NN-FUT forecasts the future effective wind, that will be used in the control scheme.

### B. DESCRIPTION OF THE VIRTUAL SENSOR

The wind speed measured by the virtual sensor is obtained in two steps. First, the sensor gives a measurement of $C_p(\lambda_i, \theta)\cdot v_{ef}^3$, that is called $CpV3_{est}$ in equations (20) and (21).

$$est_A(t_i) = \dot{w}(t_{i-1}) + (1/J) * (K_g \cdot K_\phi \cdot I_a(t_{i-1}) + K_f \cdot w(t_{i-1})) \quad (20)$$

$$CpV3_{est}(t_i) = est_A(t_i) \cdot (2 \cdot J \cdot w(t_{i-1}))/(\pi \cdot \rho \cdot R^2) \quad (21)$$

Then, the effective wind is obtained from a lookup table defined by the mapping function which relates the tuple $[v_{ef}, w, \theta]$ with the value $C_p(\lambda_i, \theta) \cdot v_{ef}^3$. This table can be obtained either by empirical experiments with the blades or by airflow simulation tools.

Figure 4 shows a representation of this lookup table for the coefficients of the wind turbine used in the experiments, when $\theta$ =0 rad and $w$ =5.4 rpm.

As it may be observed in this Figure 4, the relationship $C_p\,(\lambda_i, \theta)\cdot v_{ef}^3 \rightarrow v_{ef}$ is not one-to-one. Thus, $V_{ws}$ needs to be calculated by the procedure described below. First, we find the set of effective winds $V_{can} \subset \mathbb{R}$ whose $C_p\,(\lambda_i, \theta)\cdot v_{ef}^3$ value matches $CpV3_{est}(t_i)$ following the curve of Figure 4. Formally:

$$V_{can} \subset \mathbb{R} : \left\{ \left( v \in \mathbb{R} \mid C_p\,(\lambda_i(v, w), \theta) \cdot v^3 = CpV3_{est}\,(t_i) \right\} \quad (22)$$

Then we obtain the closest value to the previous wind speed calculated by the virtual sensor, $V_{vs}(t_{i-1})$, that is (23).

$$V_{vs}\,(t_i) = \arg MIN_{v \in V_{can}}\,(|v - V_{vs}\,(t_{i-1})|) \quad (23)$$

### C. IMPLEMENTATION OF THE CONTROLLER

The Algorithm I details the sequence of equations that are executed after the neural networks have been trained for the first time, that is, from $t > t_{onl}$ to the end of the simulation. The algorithm may help to follow the flow of the operations of equations (14-23). As it is possible to see, at each control period Tc the references are obtained, the neural networks are updated and, finally, the WT model is simulated.

Before running this algorithm, the controller calculates the reference without the use of the neural networks and a first training of the neural networks is carried out. In order to perform this first training, a dataset with $([w, \dot{w}, I_a, \theta, V_w, ], V_{vs})$ is obtained with the information from t=0 up to $t = t_{onl}$. This way, when $t > t_{onl}$ the neural networks are already trained for the first time and the Algorithm I starts.

## V. SIMULATION RESULTS

In order to show the effectiveness of the neuro control strategy, simulation experiments have been carried out with

**Algorithm 1** Execution of the controller and the model from $t > t_{onl}$

**For** $t = t_{onl}$ **to** $T_{sim}$ {
  **If** $t \geq t_{old} + T_c$ {

$V_{ACT} \leftarrow NN_{ACT}.f_{NACT}(w, \dot{w}, I_a, \theta, V_w)$
$V_{FUT} \leftarrow NN_{FUT}.f_{NFUT}(w, \dot{w}, I_a, \theta, V_w)$
$\widetilde{V_{wd}} \leftarrow K_{ACT} \cdot V_{ACT} + K_{FUT} \cdot V_{FUT}$
$\theta_{TAB} \leftarrow f_{LT}(\widetilde{V_{wd}})$
$P_{err} \leftarrow P_{ref} - P_{out}$
$\dot{P}_{err} \leftarrow (P_{ref} - P_{err})/T_c$
$sP_{err} \leftarrow sP_{err} + P_{err} \cdot T_c$
$P_{old} \leftarrow P_{err}$
$\theta_{PID} \leftarrow Kp_c \cdot P_{err} + Kd_c \cdot \dot{P}_{err} + Ki_c \cdot sP_{err}$
$\theta_{ref} \leftarrow MIN(\pi/2, MAX(0, \theta_{TAB} - \theta_{PID})$
$est_A \leftarrow \dot{w} + (1/J) * (K_g \cdot K_\phi \cdot I_a + K_f \cdot w)$
$CpV3_{est} \leftarrow est_A \cdot (2 \cdot J \cdot w)/(\pi \cdot \rho \cdot R^2)$
$V_{can} \leftarrow \left\{ (v \in \mathbb{R} | C_p(\lambda_i(v, w), \theta) \cdot v^3 = CpV3_{est} \right\} \cdot$
$V_{vs} \leftarrow \arg MIN(|v - V_{vs}|) \, | v \in V_{can}$
$NN_{ACT} \leftarrow onlineTraining(NN_{ACT}, [w, \dot{w}, I_a, \theta, V_w], V_{vs})$
$NN_{FUT} \leftarrow onlineTraining(NN_{FUT}, old[w, \dot{w}, I_a, \theta, V_w], V_{vs})$
$t_{old} \leftarrow t$
  }**endIf**
$old[w, \dot{w}, I_a, \theta, V_w] \leftarrow [w, \dot{w}, I_a, \theta, V_w]$
$[P_{out}, w, \dot{w}, I_a, \theta, V_w] \leftarrow WTmod(\theta_{ref}, V_w)$
}**endFor**

different wind profiles and several disturbance values. All the results have been obtained with the software Matlab/simulink. A variable simulation step has been used to minimize the discretization error. The maximum simulation step has been set to 10 ms and the control period Tc is 100 ms. The parameter $t_{onl}$ has been set to 10 s.

The performance of the proposed neuro-control scheme has been compared with a biased PID (24), the lookup table without the PID (with and without the neuro-estimators) (25-26), and the lookup table with the PID but without the neuro-estimators (27).

$$\theta_{ref} = \frac{\pi}{4} - \frac{\pi}{4000}[K_P \cdot P_{err} + K_D \cdot \frac{d}{dt}P_{err} + K_I \cdot \int P_{err} \cdot dt] \quad (24)$$

$$\theta_{ref} = f_{LT}(\widetilde{V_{wd}}(t)) \quad (25)$$

$$\theta_{ref} = f_{LT}(V_W(t)) \quad (26)$$

$$\theta_{ref} = f_{LT}(Vw) - \frac{\pi}{4000}[K_P \cdot P_{err} + K_D \cdot \frac{d}{dt}P_{err} + K_I \cdot \int P_{err} \cdot dt] \quad (27)$$

The range of the pitch reference is [0, $\pi$/2] rad. Thus, the bias of the PID has been assigned half the input range, i.e., $\pi$/4. The PID tuning parameters [$K_P$, $K_D$, $K_I$] have been obtained by trial and error; their values are [1, 0.2, 0.1], respectively.

To test the control approaches, the following metrics have been used: MSE [W] and Mean [W] (28-29).

$$MSE[W] = \sqrt{\frac{1}{T_{sim}} \sum_i \left[ \left( P_{out}(t_i) - P_{ref} \right)^2 T_s(t_i) \right]} \quad (28)$$

$$Mean[W] = \frac{1}{T_{sim}} \sum_i [P_{out}(t_i) \cdot T_s(t_i)] \quad (29)$$

The values of the parameters used during the simulation are shown in Table 1, taken from [26] for a 7 kW turbine.

**TABLE 1. Parameters of the wind turbine model [26].**

| Symbol | Quantity | Value/Units |
|---|---|---|
| $L_a$ | Inductance of the armature | 13.5 mH |
| $K_g$ | Constant of the generator | 23.31 |
| $K_\phi$ | Magnetic flow coupling constant | 0.264 V/rad/s |
| $R_a$ | Resistance of the armature | 0.275 Ω |
| $R_L$ | Resistance of the load | 8 Ω |
| $J$ | Inertia | 6.53 Kg m$^2$ |
| $R$ | Radius of the blade | 3.2 m |
| $\rho$ | Density of the air | 1.223 Kg/m$^3$ |
| $K_f$ | Friction coefficient | 0.025 N m/rad/s |
| $[c_1, c_2, c_3]$ | $C_p$ constants | $[0.73, 151, 0.58]$ |
| $[c_4, c_5, c_6]$ | $C_p$ constants | $[0.002, 2.14, 13.2]$ |
| $[c_7, c_8, c_9]$ | $C_p$ constants | $[18.4, -0.02, -0.003]$ |
| $[K_\theta, T_\theta]$ | Pitch actuator constants | $[0.15, 2]$ |

The control approaches have been evaluated with different wind profiles: constant, random, sinusoidal, square, ramp and sawtooth. The range of the wind speed is between 11 to 13 m/s. The modelled wind turbine has a rated wind speed of 12.25 m/s, which means that below this cut-off speed the wind power is not enough to generate 7kW. Thus, the pitch control only works when wind speed is over this value. This range of winds speeds reflect the reality. Indeed, they correspond to "Strong breeze" regarding the Beafourt scale. Velocities from 11 to 13 m/s, that is, 21 to 25 kts, are typical in a windy day in many places, for example in the North of Spain, where some wind turbines are installed.

The random wind speed oscillates between 12.25 and 12.75 m/s. The sinusoidal wind has a mean value of 12.5 m/s, an amplitude of 1 m/s and a time period of 50 s. The ramp has a slope of 0.01 m/s and a start value of 11 m/s. The square wave switches between 12.15 m/s and 13.1 m/s of amplitude with a time period of 50 s. Finally the sawtooth profile has limits at 12.25 and 13.1 m/s, and a time period of 50 s.

### A. PERFORMANCE WITHOUT EXTERNAL DISTURBANCES

Figure 5 shows the comparison of the output power when the different control strategies are applied. The wind speed is a random value between 12.25 and 12.75 m/s.

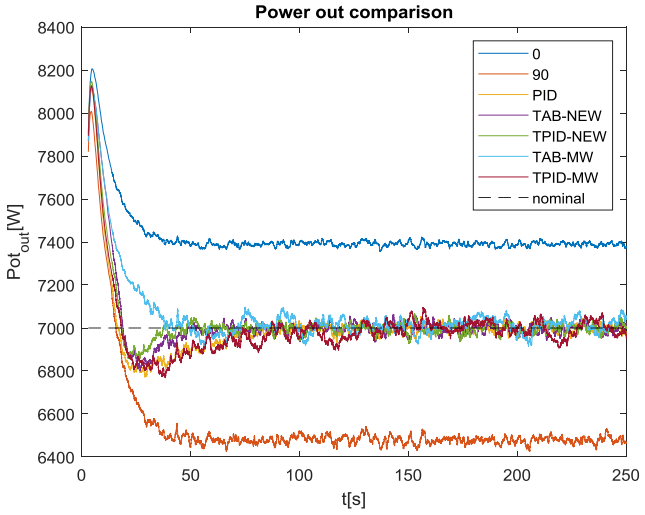


**FIGURE 5.** Comparison of output power for different control techniques with random wind without external disturbance.

In the following figures, the color code is as follows. The dark blue line represents the output when the pith reference is permanently set to 0° and the red one when it is set to 90°. The yellow line is the output power with the PID controller and the purple one is the output when the pitch is only determined by the lookup table and the effective wind is estimated by the neural network (TAB-NEW). The green line is the output power when the pitch is determined by the lookup table together with a PID and the wind is estimated by the neural network (TPID-NEW). The output power when the pitch is obtained by only the lookup table and the wind is measured only by the sensor is represented in light blue (TAB-MW). The magenta line represents the output when the pitch is determined by the lookup table together with a PID but the wind is only measured by the sensor (TPID-MW). Finally, the black dashed line is the rated power.

As expected, pitch angle 0° and 90° configurations provide the maximum and minimum power, respectively. It is also possible to observe how all the controllers stabilize the output power around the rated value. However, TPID-NEW configuration gives the smallest settling time. Although external disturbances have not been considered in this experiment, the results of TAB-NEW and TAB-MW are not the same due to the effect of the internal disturbance (12).

Figure 6 shows the pitch of the blades for each control strategy. The color code is the same as in Figure 5. It is noticeable how the pitch angles obtained by TAB-MW and TPID-MW are the noisiest. A possible explanation of this effect is that these techniques do not include the neuro-estimator that tends to smooth the pitch reference.

Figure 7 shows the comparison of the output power when the wind follows a sawtooth profile with limits at 12.25 and

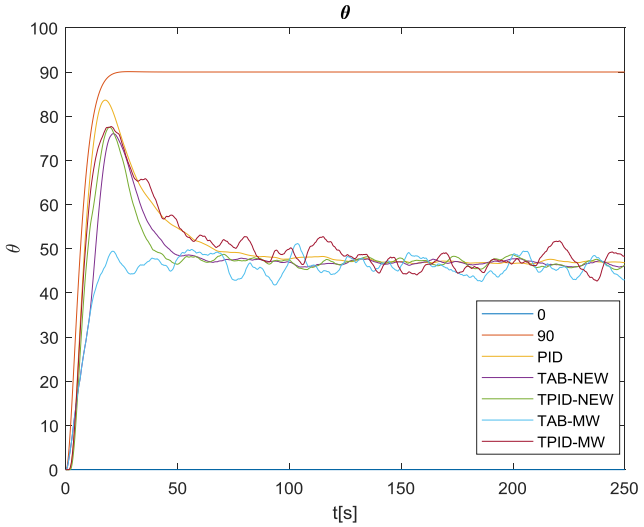


**FIGURE 6.** Comparison of pitch signal for different control techniques with random wind without external disturbance.

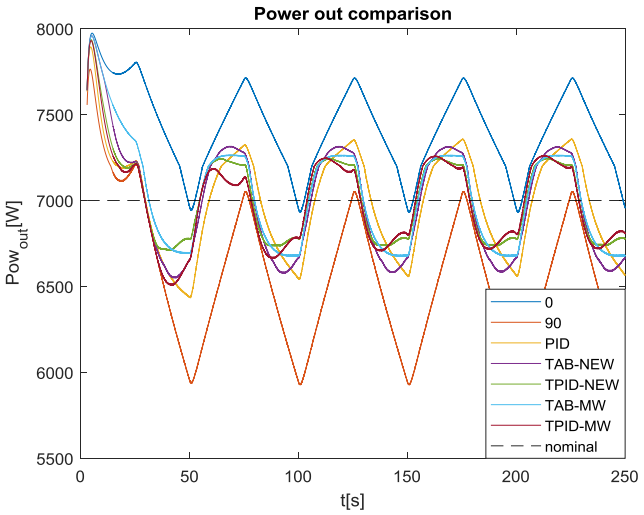


**FIGURE 7.** Comparison of output power for different control techniques with sawtooth wind without external disturbance.

13.1 m/s, and a time period of 50 s. This sawtooth shape is clearly observable in the output power when the pitch is set to 0° and 90°. However, the other control strategies limit the peaks and the output power has a more trapezoid shape. The TPID controller with the neuro estimators provides the minimum error.

The pitch signal of this experiment is shown in Figure 8. The periodic behavior of the output power can also be observed in the pitch signal but in this case with a sinusoidal shape. TPID-NEW and TPID-MW are similar but not exactly the same due to the fact that there are not external disturbances.

In addition to the graphical results, numerical outcomes have been obtained. Tables 2 and 3 show the comparison of the MSE and mean values of the output power when the proposed control strategies have been applied with

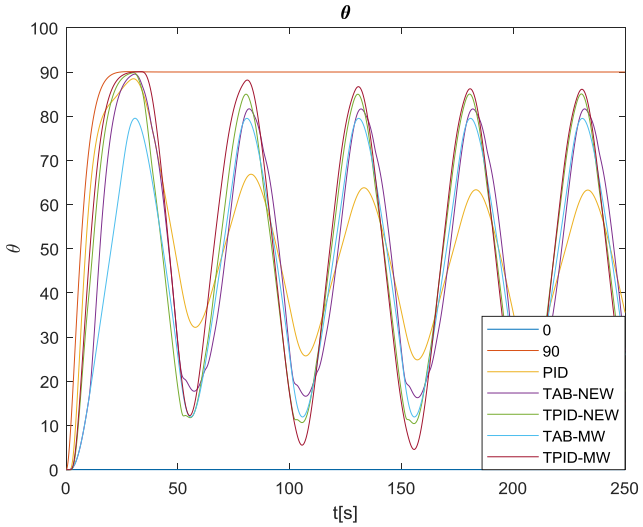


**FIGURE 8.** Comparison of pitch signal for different control techniques with sawtooth wind without external disturbance.

**TABLE 2.** Comparison of MSE [W] for different controllers without external disturbance.

| Wind type | PID | TAB NE-Wind | TPID NE-Wind | TAB M-Wind | TPID M-Wind |
|---|---|---|---|---|---|
| 12.25 | 152.08 | 156.39 | **140.01** | 164.83 | 140.12 |
| 12.75 | **182.22** | 187.44 | **182.22** | 193.82 | 188.72 |
| Random | **169.87** | 185.58 | 172.22 | 194.33 | 175.49 |
| Sine | 406.12 | 350.31 | **307.34** | 350.31 | 352.87 |
| Ramp | 469.80 | 449.39 | **447.75** | 449.75 | 454.57 |
| Square | 443.95 | 418.11 | 401.77 | 397.13 | **386.60** |
| Sawtooth | 301.80 | 327.87 | **253.66** | 300.58 | 264.11 |

**TABLE 3.** Comparison of mean value [kW] for different controllers without external disturbance.

| Wind type | PID | TAB NE-Wind | TPID NE-Wind | TAB M-Wind | TPID M-Wind |
|---|---|---|---|---|---|
| 12.25 | 6.97 | 7.01 | 7.01 | 7.05 | **7,00** |
| 12.75 | **7.01** | 7.03 | **7.01** | 7.05 | **6.99** |
| Random | **7.00** | 7.02 | 7.02 | 7.06 | 6.99 |
| Sine | **6.97** | 6.95 | 6.96 | **6.97** | **6.97** |
| Ramp | **6.80** | 6.76 | 6.75 | 6.76 | 6.77 |
| Square | 7.01 | **7.00** | **7.00** | 7.03 | **7.00** |
| Sawtooth | **6.99** | **6.99** | **7.01** | 7.03 | **6.99** |

different wind profiles. The random and sawtooth wind profiles have the same characteristics as in the experiments of Figures 5 and 7.

In the columns of these Tables, the term TAB represents the values obtained when the lookup table is used without PID. The term TPID indicates the values obtained when the lookup table is used together with the PID. On the other hand, NE-wind represents that the wind speed is obtained by the neural estimators and M-wind refers to wind values measured directly by the sensor.

Although in these experiments external disturbances have not been included, the TPID with the neuro-estimated wind provides the smallest MSE for almost all wind profiles. It is also possible to see how, in general, the combination of TAB and PID provides better results than the individual application of each technique, even when the wind is measured. However, the best mean values are provided by the PID and the TPID with measured wind. The control approach TPID-NE provides an improvement of 24% for sinusoidal wind and an average improvement of 10% respect to the PID.

In order to facilitate the comparison of the results, Figure 9 shows the MSE for all the control strategies. It is possible to see how the best performance is obtained by the proposed new control scheme TPID-NE, and the best improvements are achieved with sinusoidal and sawtooth wind profiles.

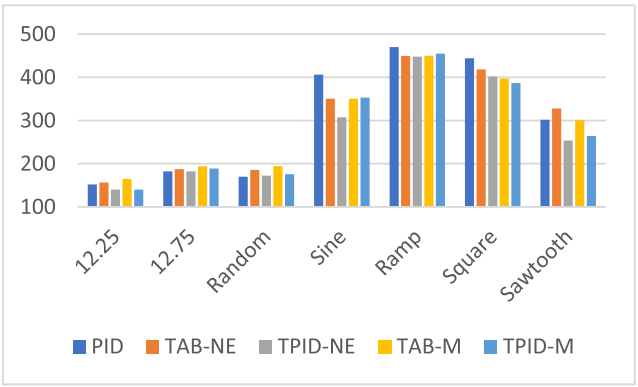


**FIGURE 9.** Comparison of MSE [W] for the different control strategies without external disturbance.

### B. WIND AND DISTURBANCE ESTIMATION

In previous experiments the external disturbance has been discarded to see how the control systems performs. Now, in the following experiment an external disturbance has been included, with a sinusoidal shape with 0.3 m/s mean value, 0.3 m/s of amplitude and a time period of 30 s. A random signal of 0.3 m/s is also added to this disturbance. The measured wind has the sawtooth profile used before. The neural estimators are trained from the beginning of the simulation up to t=10 s, then the on-line learning algorithm is applied up to the end.

Figure 10 shows the wind measured by the sensor in yellow, the combination of the wind and the disturbance in red, the effective wind estimated by the neural estimator in green; the future effective wind predicted by the neural estimator is represented by the blue line.

It is worth noting the sinusoidal influence of the disturbance in the input wind. As expected, the measured wind has a sawtooth shape. It is also possible to observe how the estimation of the current wind fits quite well the input wind. In general, it is possible to say that the future wind is well predicted by the neuro-estimator, although some peaks appear when the slope of the measured wind changes from negative to positive values. Despite these peaks, as it will be seen in

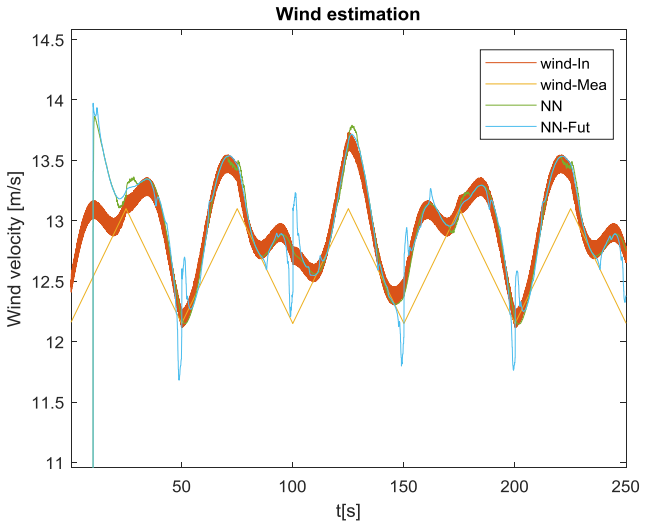


**FIGURE 10.** Effective wind estimation when wind type is sawtooth and there is a sinusoidal external disturbances.

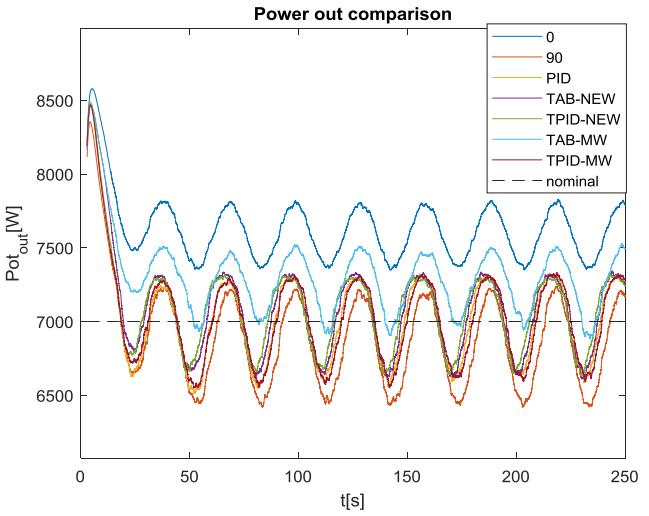


**FIGURE 12.** Comparison of output power for different control techniques with random wind and external disturbance.

the next section, the performance of the controller is better when the future estimation is considered.

The estimation of the disturbance for the same experiment is shown in Fig 11. The blue line represents the disturbance, the yellow one is the current disturbance neuro-estimated and the purple line shows the future disturbance predicted by the neuro-estimator. The disturbance is a sinusoidal signal with random noise. The width of the line shows the noise level of the signal. As in Figure 10, the estimation at the current time fits quite well the expected value, however the future forecasting shows peaks at the same instants of time as before.

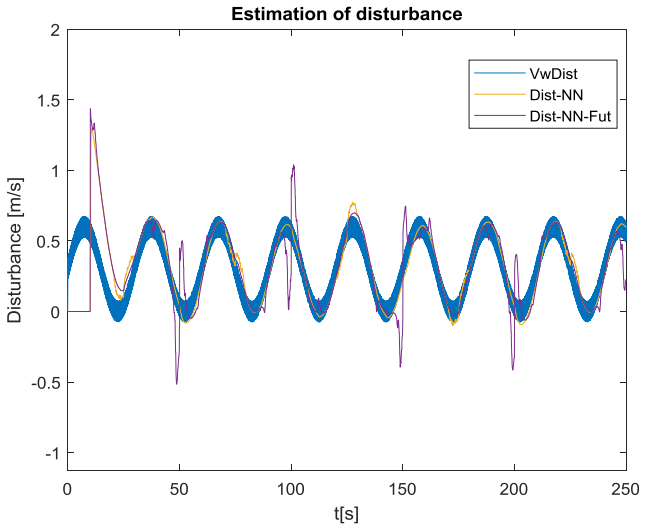


**FIGURE 11.** Disturbance estimation when wind type is sawtooth and there is a sinusoidal external disturbance.

### C. PERFORMANCE WITH EXTERNAL DISTURBANCES

In the next experiment the input wind is randomly generated between 12.25 and 12.75 m/s, and an external disturbance with the same characteristics as in the previous section is included. Figure 12 shows the comparison of the output power when different control strategies are applied. The color code is the same as in Figure 5.

As expected, the worst results are obtained with 0° and TAB-MW control strategy. The disturbance increases the mean value of the effective wind. This produces a bigger output power, therefore a higher pitch value is needed to compensate it. However, the lookup table with the measured wind as input does not perceive this increment in the effective wind and it generates a pitch angle smaller than the necessary one.

The amplitude of the disturbance pushes the WT to its regulation limits so the effect of the disturbance cannot be completely eliminated. Despite this issue, it is still possible to observe how the best performance is obtained with the TPID-NEW strategy.

In order to better analyse these results (Figure 12), the numeric values of the MSE and the mean value of the output power are shown and compared in Tables 4 and 5. The description of each column is the same as in previous tables. In this case, it is clear that TPID with neuro-estimated wind gives the lowest MSE for all the tested wind profiles. It is also remarkable that the use of neuro-estimated wind gives better results with the TAB controller (comparison between third and fifth columns in Table 4 ). Another relevant result is that the use of TPID, even with measured wind, improves the control performance respect to the use of the PID (comparison between the second and the last columns in Table 4). In this case the improvement achieved with the different control approaches for different wind profiles is more similar than the one previously obtained in Table 2. Again the best results is obtained by the TPID-NE control strategy (16% improvement for sinusoidal wind and an average improvement of 8% respect to the PID).

**TABLE 4. Comparison of MSE [W] for different controllers with external disturbance.**

| Wind type | PID | TAB NE-Wind | TPID NE-Wind | TAB M-Wind | TPID M-Wind |
|---|---|---|---|---|---|
| 12.25 | 320.65 | 354.36 | **314.38** | 399.84 | 315.09 |
| 12.75 | 346.24 | 349.83 | **335.88** | 405.71 | 346.76 |
| Random | 337.35 | 349.03 | **326.10** | 403.39 | 338.09 |
| Sine | 480.74 | 425.14 | **401.41** | 453.38 | 435.70 |
| Ramp | 409.73 | 387.51 | **384.04** | 409.72 | 387.02 |
| Square | 501.09 | 488.53 | **462.34** | 506.53 | 481.18 |
| Sawtooth | 405.47 | 402.31 | **358.30** | 435.85 | 382.74 |

**TABLE 5. Comparison of mean value [kW] for different controllers with external disturbance.**

| Wind type | PID | TAB NE-Wind | TPID NE-Wind | TAB M-Wind | TPID M-Wind |
|---|---|---|---|---|---|
| 12.25 | **6,99** | 7,03 | 7,02 | 7,31 | 7,03 |
| 12.75 | 7,04 | 7,12 | 7,14 | 7,3 | **7,03** |
| Random | **7,02** | 7,09 | 7,09 | 7,3 | 7,03 |
| Sine | 7,03 | 7,08 | 7,08 | 7,25 | **7,02** |
| Ramp | 6,96 | 6,95 | 6,95 | 7,06 | **6,99** |
| Square | **7,04** | 7,15 | 7,15 | 7,29 | 7,08 |
| Sawtooth | **7,02** | 7,10 | 7,12 | 7,29 | 7,03 |

However, in view of the values of Table 5, the best output power mean values are obtained with the PID controller followed by the TPID M-Wind strategy. A possible explanation of this outcome is that the PID does not use the wind values in the control law but only the power errors; this produces more symmetric values respect to the rated power.

Figure 13 shows these results for all the control strategies. The best performance is obtained with the proposed TPID-NE control for sinusoidal and sawtooth wind profiles. Comparing this figure with Figure 9, it is possible to see that the worst performance corresponds to the TAB-M control. This may be explained due to the fact that the PID is not directly affected by the disturbance in the measurement of the wind as the TAB-M approach is.

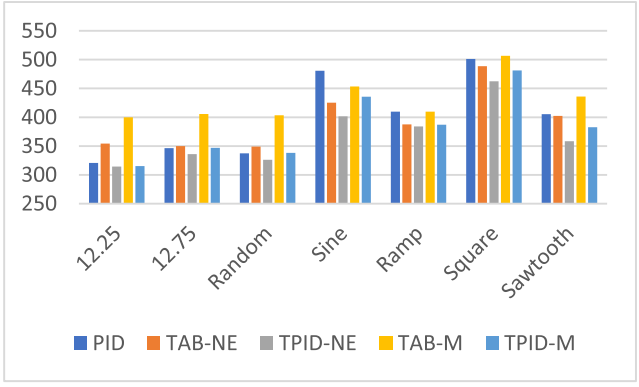


**FIGURE 13. Comparison of MSE [W] for the different controllers with external disturbance.**

### D. INFLUENCE OF THE PERIOD OF THE EXTERNAL DISTURBANCE

In the next experiment the effect of the time period of the disturbance is evaluated. To do it, different simulations are carried out with a sawtooth reference defined as in Figure 7, a sinusoidal disturbance of 0.3 m/s mean value, amplitude of 0.3 m/s and a different period each time. The period value varies between 0 and 100 s. These values are standard in the ocean waves. For each simulation the MSE of the output power is calculated.

The result of this experiment is shown in Figure 14. The blue line represents the MSE values with the PID and the red one is the MSE values obtained with the TPID with neuro-estimated wind. In the case of the PID, it may be observed how the MSE increases with the period of the disturbance, with some exceptions (at periods of 40 s and 80 s). However, in the case of the TPID-NEW control the MSE increases up to period of 20 s, and from then on a decreasing trend is observable. A possible explanation of this effect is that the high frequency external disturbances are filtered by the wind turbine and only its mean value affects the MSE. When the period grows, the variation of the disturbance cannot be filtered and their influence on the output power is larger. On the other hand, slower disturbances are better estimated, thus they can be considered by the TPID-NEW and its influence is reduced. In all cases the performance of TPID-NEW control scheme is better than the PID controller.

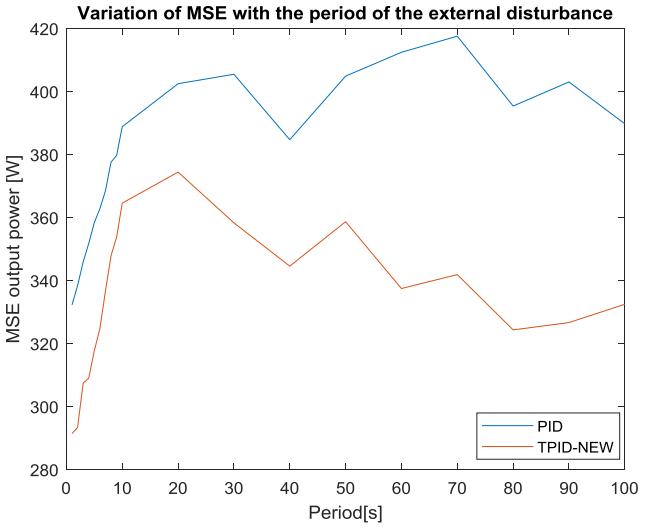


**FIGURE 14. Variation of MSE with the period of the external disturbance for a sawtooth wind.**

### E. INFLUENCE OF THE RELATIONSHIP BETWEEN ESTIMATION AND FORECASTING

Finally, the influence of the parameter $K_{FUT}$ is studied to see the benefits of considering the future wind. Several simulations for all the different wind profiles considered in Table 4 have been carried out. In all the cases a disturbance as in Figure 12 is introduced. For each wind profile the parameter

$K_{FUT}$ varies from 0 to 1. The $K_{ACT}$ parameter is set to $1 - K_{FUT}$. For each simulation the MSE is obtained. The average MSE of each $K_{FUT}$ for all the simulations is shown in Figure 15.

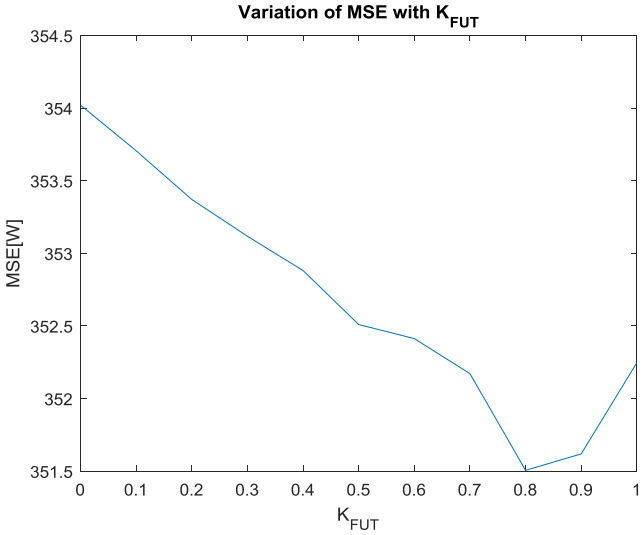


**FIGURE 15.** Variation of the average MSE of the output power with the $K_{FUT}$ parameter.

The behaviour of Figure 15 shows a clear decreasing trend up to $K_{FUT}$ is 0.8, where there is a local minimum. As observed it is positive to consider the forecasting of the wind in the control of the output power. In the previous experiments this parameter had been set to 0.5, in order to give the same weight to the actual estimation and the future prediction.

## VI. CONCLUSION AND FUTURE WORKS

Considering the effective wind speed allows to achieve relevant improvements in the performance of the control of a wind turbine. However, the effective wind speed, that is, the speed of the wind that really impacts the rotor and is transformed into mechanical power, cannot be directly measured by a sensor such as an anemometer. In addition, the turbine blades act as a filter. This makes the effective wind different from that measured externally. On the other hand, WTs are subject to oscillations and vibrations that distort the external wind measurement, an effect that is even more noticeable in floating offshore wind turbines since they are subject to extreme external conditions.

To address this problem, in this work the use of a neuro-estimator based on neural networks is proposed with the objective of estimating the effective wind and predicting the wind in the next control period. Both signals, the current wind and the forecasting wind, are included in the controller. The proposed control architecture combines a PID and a look-up table, and a neural network that estimates the effective wind, and a virtual sensor. The neural estimator consists of two neural networks, one for estimating and one for predicting the wind speed. Neural networks are trained online to allow them to react to changes in the environment, wind conditions or even variations in the WT dynamics.

The results of the different simulated experiments validate the efficiency of the proposed intelligent control approach. This neural controller scheme is compared to a PID, giving better results.

As future work, it would first be desirable to test the proposal on a real prototype of a wind turbine. Also, it would be interesting to apply this control strategy to a larger turbine. To do so, the small wind turbine is going to be scaled to a bigger one. This will allow us to analyze the sensitivity of the model when the parameters (size, mass, mechanical and electrical components) vary. In addition, this will allow us to see if this control action affects the stability of a floating offshore wind turbine.

## ACKNOWLEDGMENT

This work was partially supported by the Spanish Ministry of Science, Innovation and Universities under MCI/AEI/FEDER Project number RTI2018-094902-B-C21.

## REFERENCES

[1] Paris, France. (2020). *Climate*. Accessed: Dec. 4, 2020. [Online]. Available: https://ec.europa.eu/clima/policies/international/negotiations/paris_en

[2] International Renewable Energy Agency, Abu Dhabi, United Arab Emirates. (2019). *Future of Wind: Deployment, Investment, Technology, Grid Integration and Socio-Economic Aspects (A Global Energy Transformation Paper*. [Online]. Available: https://www.irena.org/-/media/Files/IRENA/Agency/Publication/2019/Oct/IRENA_Future_of_wind_2019.pdf

[3] M. Tomás-Rodríguez and M. Santos, "Modelling and control of floating offshore wind turbines," *Revista Iberoamericana de Automática e Informática Ind.*, vol. 16, no. 4, pp. 381–390, 2019.

[4] J. E. Sierra-García and M. Santos, "Performance analysis of a wind turbine pitch neurocontroller with unsupervised learning," *Complexity*, vol. 2020, pp. 1–15, Sep. 2020.

[5] J. E. Sierra-García and M. Santos, "Exploring reward strategies for wind turbine pitch control by reinforcement learning," *Appl. Sci.*, vol. 10, no. 21, p. 7462, Oct. 2020.

[6] Y. Wang, Y. Yu, S. Cao, X. Zhang, and S. Gao, "A review of applications of artificial intelligent algorithms in wind farms," *Artif. Intell. Rev.*, vol. 53, no. 5, pp. 3447–3500, Jun. 2020.

[7] E. C. Navarrete, M. T. Perea, J. C. J. Correa, R. V. C. Serrano, and G. J. R. Moreno, "Expert control systems implemented in a pitch control of wind turbine: A review," *IEEE Access*, vol. 7, pp. 13241–13259, 2019.

[8] P. M. Rubio, J. F. Quijano, and P. Z. López, "Intelligent control for improving the efficiency of a hybrid semi-submersible platform with wind turbine and wave energy converters," *Revista Iberoamericana de Automática e Informática Industrial*, vol. 16, no. 4, pp. 480–491, 2019.

[9] E. Chavero-Navarrete, M. Trejo-Perea, J. C. Jáuregui-Correa, R. V. Carrillo-Serrano, G. Ronquillo-Lomeli, and J. G. Ríos-Moreno, "Hierarchical pitch control for small wind turbines based on fuzzy logic and anticipated wind speed measurement," *Appl. Sci.*, vol. 10, no. 13, p. 4592, Jul. 2020.

[10] B. Xu, Y. Yuan, H. Liu, P. Jiang, Z. Gao, X. Shen, and X. Cai, "A pitch angle controller based on novel fuzzy-PI control for wind turbine load reduction," *Energies*, vol. 13, no. 22, p. 6086, Nov. 2020.

[11] A. B. Asghar and X. Liu, "Adaptive neuro-fuzzy algorithm to estimate effective wind speed and optimal rotor speed for variable-speed wind turbine," *Neurocomputing*, vol. 272, pp. 495–504, Jan. 2018.

[12] F. Yao, W. Liu, X. Zhao, and L. Song, "Integrated machine learning and enhanced statistical approach-based wind power forecasting in australian tasmania wind farm," *Complexity*, vol. 2020, pp. 1–12, Sep. 2020.

[13] A. B. Asghar and X. Liu, "Estimation of wind speed probability distribution and wind energy potential using adaptive neuro-fuzzy methodology," *Neurocomputing*, vol. 287, pp. 58–67, Apr. 2018.

[14] X. Deng, J. Yang, Y. Sun, D. Song, Y. Yang, and Y. H. Joo, "An effective wind speed estimation based extended optimal torque control for maximum wind energy capture," *IEEE Access*, vol. 8, pp. 65959–65969, 2020.
[15] X. Deng, J. Yang, Y. Sun, D. Song, X. Xiang, X. Ge, and Y. H. Joo, "Sensorless effective wind speed estimation method based on unknown input disturbance observer and extreme learning machine," *Energy*, vol. 186, Nov. 2019, Art. no. 115790.
[16] A. Saenz-Aguirre, E. Zulueta, U. Fernandez-Gamiz, J. Lozano, and J. Lopez-Guede, "Artificial neural network based reinforcement learning for wind turbine yaw control," *Energies*, vol. 12, no. 3, p. 436, Jan. 2019.
[17] M. Bahaghighat, Q. Xin, S. A. Motamedi, M. M. Zanjireh, and A. Vacavant, "Estimation of wind turbine angular velocity remotely found on video mining and convolutional neural network," *Appl. Sci.*, vol. 10, no. 10, p. 3544, May 2020.
[18] H. S. Dhiman and D. Deb, "Wake management based life enhancement of battery energy storage system for hybrid wind farms," *Renew. Sustain. Energy Rev.*, vol. 130, Sep. 2020, Art. no. 109912.
[19] H. S. Dhiman, D. Deb, and A. M. Foley, "Bilateral Gaussian wake model formulation for wind farms: A forecasting based approach," *Renew. Sustain. Energy Rev.*, vol. 127, Jul. 2020, Art. no. 109873.
[20] R. I. Cortez and J. R. Dorrego, "Analysis of the wake effect in the distribution of wind turbines," *IEEE Latin Amer. Trans.*, vol. 18, no. 4, pp. 668–676, Apr. 2020.
[21] M. A. Mohamed, A. A. Z. Diab, H. Rezk, and T. Jin, "A novel adaptive model predictive controller for load frequency control of power systems integrated with DFIG wind turbines," *Neural Comput. Appl.*, vol. 32, no. 11, pp. 7171–7181, Jun. 2020.
[22] M. A. Mohamed, T. Jin, and W. Su, "An effective stochastic framework for smart coordinated operation of wind park and energy storage unit," *Appl. Energy*, vol. 272, Aug. 2020, Art. no. 115228.
[23] I. L. R. Gomes, R. Melicio, V. M. F. Mendes, and H. M. I. Pousinho, "Wind power with energy storage arbitrage in day-ahead market by a stochastic MILP approach," *Log. J. IGPL*, vol. 28, no. 4, pp. 570–582, Jul. 2020.
[24] M. Mikati, M. Santos, and C. Armenta, "Modelado y simulación de un sistema conjunto de energía solar y eólica para analizar su dependencia de la red eléctrica," *Revista Iberoamericana de Automática e Informática Ind.*, vol. 9, no. 3, pp. 267–281, Jul. 2012.
[25] W. H. Munk, *Origin and Generation of Waves*. La Jolla, CA, USA: Scripps Institution of Oceanography, 1951.
[26] M. Mikati, M. Santos, and C. Armenta, "Electric grid dependence on the configuration of a small-scale wind and solar power hybrid system," *Renew. Energy*, vol. 57, pp. 587–593, Sep. 2013.

**J. ENRIQUE SIERRA-GARCÍA** was born in Burgos, Spain. He received the M.Sc. degree in electronics from the University of Valladolid (UVA), in 2007, the M.Sc. degree in control engineering from the National University for Distance Education (UNED), in 2014, the M.Sc. degree in telecommunications from the University of Valladolid (UVA), in 2015, and the Ph.D. degree in computer science, in 2019. Since 2012, he has been with the University of Burgos, where he is currently a Lecturer in system engineering and automatic control with the Department of Electromechanical Engineering. He is the Founder of the Joint Research Unit ASTI-UBU on autonomous vehicles, mobile robotics, and AGVs. He has been a Principal Researcher in 15 research projects related with mobile robotics. In addition, his professional experience includes 15 years working as a Researcher and a Software and Hardware Engineer in several companies. His major research interests include intelligent control, robotics, autonomous guided vehicles, modeling, simulation, and wind energy.

**MATILDE SANTOS** was born in Madrid, Spain. She received the B.Sc. and M.Sc. degrees in physics (computer engineering) and the Ph.D. degree in physics from the University Complutense of Madrid (UCM). She is currently a Full Professor in system engineering and automatic control. She is a member of the European Academy of Sciences and Arts. She has published many articles in international scientific journals and several books and book chapters. She has supervised more than ten Ph.D. students. She has worked on several national, European, and international research projects, leading some of them. She currently serves as a member on the Editorial Board of prestigious journals. She is an Editor-In-Chief Assistant of one of them. Her major research interests include intelligent control (fuzzy and neuro-fuzzy), pattern recognition, modeling and simulation, and wind energy.